© 2003 The Chemical Society of Japan

Selective Formation and Characterization of Oxorhenium(V) Complexes with 2-Methylquinolin-8-ylamido (Hamq). Interconversion between $[ReOX_2(Hamq)(PPh_3)]$ and $[ReOX_2(Hamq)(OPPh_3)]$ (X = Cl, Br)

Tetuya Ohashi, Yoshitaro Miyashita,* Yasunori Yamada,# Kiyoshi Fujisawa, and Ken-ichi Okamoto*

Department of Chemistry, University of Tsukuba, Tsukuba 305-8571

(Received December 17, 2002)

The reactions of Re(V) precursors $[ReOX_3(PPh_3)_2]$ (X = Cl, Br) with 8-amino-2-methylquinoline (H_2amq) gave $[ReOX_2(Hamq)(PPh_3)]$ (X = Cl, **1**; Br, **2**) as major products and $[ReOX_2(Hamq)(OPPh_3)]$ (X = Cl, **3**; Br, **4**) as minor products. **3** and **4** were also obtained from the reaction of **1** and **2** with an excess of free $OPPh_3$ ligand. The crystal structures of **1**, **3**, and **4** were determined by X-ray analyses. These complex molecules have a distorted octahedral geometry. The Re=O bond in **1** occupies the *trans* position to the amido N atom of the partially deprotonated H_2amq ligand. Its distance (1.724(4) Å) is long due to the *trans* influence of the amido N atom. The Re=O bonds in **3** and **4** occupy the *trans* position to the O atom of the $OPPh_3$ ligand, indicating a geometrical conversion during the ligand substitution reaction. Some intramolecular and/or intermolecular stacking interactions are also observed in the crystalline state. All complexes were characterized in the solid state by IR, far-IR, diffuse reflectance, and $^{31}P\{^1H\}$ CP-MAS NMR spectra. From UV-vis absorption and $^{31}P\{^1H\}$ NMR spectra, it was indicated that the PPh_3 and $OPPh_3$ ligands in **1**–**4** are released in solution.

Rhenium compounds containing an oxorhenium(V) core have been of interest in nuclear medical theraphy.[1] In addition, the oxorhenium(V) core has many other attractive features, such as its oxygen transfer properties, catalytic processes, spectroscopy, and coordination geometry.[2–7] Therefore, it is important to explore the stereoselective synthesis and reactivity. In recent years, the nitrogen-containing Re(V) complexes, which have monodentate-*N* ligands or didentate-*N*,*N* ligands, have been widely investigated.[7–13] Many symmetrical didentate-*N*,*N* ligands, such as bipyridine[12,13] and biimidazole,[10,11] have received special attention. When the coordinated nitrogen atom is part of an arylamino group, furthermore, the deprotonated monodentate imido ligand imitates the features of a multiple Re–N bond between double and triple bonds, depending on the Re–N–C bond angle.[14–20] Therefore, 8-aminoquinoline (H_2aq), which has two types of nitrogen atoms in a heterocyclic ring and an aromatic amine, is favorable as the didentate-*N*,*N* ligand from the standpoint of fixing the bond angle of the imido ligand. In 1995, Ahmet et al. reported that two equivalents of H_2aq reacted with an oxorhenium(V) precursor $[ReOCl_3(PPh_3)_2]$ as a didentate quinolinylamido (amino group is partially deprotonated) to form $[ReO(Haq)_2(PPh_3)]BPh_4$.[14] On the other hand, we have recently reported that one equivalent of H_2aq reacted with the oxorhenium(V) precursor as a didentate quinolinylimido (amino group is fully deprotonated) deoxidized the oxorhenium(V) core to form $[ReCl_3(aq)(PPh_3)]$.[20] It occurred to us that closer exploration was necessary to describe these properties.

In the present work, we introduced a 2-methyl derivative, 8-amino-2-methylquinoline (H_2amq), as the unsymmetrical bidentate-*N*,*N* ligand and attempted to synthesize the corresponding two types of Re(V) complexes; $[ReO(Hamq)_2(PPh_3)]^+$ and $[ReCl_3(amq)(PPh_3)]$. In practice, however, new types of complexes were obtained. Moreover, they showed a very interesting replacement reaction that lead to changing coordination geometry. We describe here the systematical synthesis, characterization, and coordination geometrical change around the oxorhenium(V) core. The interconversion between $[ReOX_2(Hamq)(PPh_3)]$ and $[ReOX_2(Hamq)(OPPh_3)]$ (X = Cl, Br) is also discussed on the basis of X-ray crystal structures and some spectroscopic analyses (Chart 1).

Results and Discussion

Syntheses and Reactivity. The reactions of the oxorhenium(V) precursors $[ReOX_3(PPh_3)_2]$ (X = Cl, Br) with 8-amino-2-methylquinoline (H_2amq) as a 1:2 molar ratio in the $CH_2Cl_2/C_6H_5CH_3$ mixed solvent gave selectively the dark

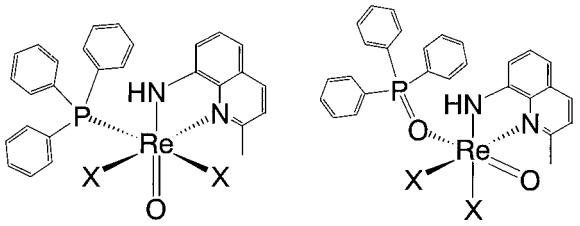

$[ReOX_2(Hamq)(PPh_3)]$ X = Cl, **1**; Br, **2**

$[ReOX_2(Hamq)(OPPh_3)]$ X = Cl, **3**; Br, **4**

Chart 1.

Present Address: Department of Chemistry, Faculty of Science and Engineering, Saga University, Saga 840-8502

brown precipitate $[ReOX_2(Hamq)(PPh_3)]$ (X = Cl, **1**; Br, **2**) (Eq. 1). In spite of the addition of two equivalents of H_2amq, no complexes containing two amq ligands, such as $[ReO(Hamq)_2(PPh_3)]^+$, could be obtained. Since the bis type complex $[ReO(Haq)_2(PPh_3)]^+$ was obtained from the reaction with an excess of H_2aq,[14] H_2amq and H_2aq seem to extract the halide ions from the oxorhenium(V) precursors.

$$[ReOX_3(PPh_3)_2] + 2H_2amq \longrightarrow [ReOX_2(Hamq)(PPh_3)] + PPh_3 + H_3amqX \quad (1)$$
X = Cl, **1**; Br, **2**

The recrystallization of the dark brown precipitate gave two types of crystals. Although most of them were the dark brown prismatic-shaped crystals, the small amounts of dark brown octahedral-shaped crystals were also formed. From X-ray analyses and IR spectra, the major crystals were the PPh_3 complexes $[ReOX_2(Hamq)(PPh_3)]$ (X = Cl, **1**; Br, **2**), whereas the minor crystals were the $OPPh_3$ complexes $[ReOX_2(Hamq)(OPPh_3)]$ (X = Cl, **3**; Br, **4**). Specifically, it seems that oxidation and ligand substitution reactions of PPh_3 with $OPPh_3$ occurred during the recrystallization. The $OPPh_3$ complexes **3** and **4** can also be synthesized by the reaction of **1** and **2** with an excess of free $OPPh_3$. These reactions can be reversed from **3** and **4** to **1** and **2** by adding an excess of free PPh_3 (Eq. 2).

$$[ReOX_2(Hamq)(PPh_3)] + OPPh_3 \rightleftharpoons [ReOX_2(Hamq)(OPPh_3)] + PPh_3 \quad (2)$$
X = Cl, **1**; Br, **2** — X = Cl, **3**; Br, **4**

Although **1**–**4** are stable in the solid state even under aerobic atmosphere, it is suspected that they release PPh_3 or $OPPh_3$ in solution from the UV-vis absorption and $^{31}P\{^1H\}$ NMR spectra. In the present case, therefore, it is conceivable that the PPh_3 complexes (**1** and **2**) and/or the $OPPh_3$ complexes (**3** and **4**) precipitate depending on the amount of free PPh_3 or $OPPh_3$ in solution. Namely, these complexes showed the easy substitution reaction of PPh_3 by $OPPh_3$. Additionally, it is suggested that **3** and **4** were produced as the minor products from the reactions of **1** and **2** with a small amount of $OPPh_3$, which was formed by the oxidation of free PPh_3, during the recrystallization. Since the corresponding 2-methyl-8-quinolinolato (hmq) complex $[ReOCl_2(hmq)(PPh_3)]$, which was synthesized by the same method to **1** using Hhmq instead of H_2amq, is stable in solution and shows no reaction with $OPPh_3$,[21] it can be said that the present easy substitution property is very interesting. Indeed, many reported Re(V) complexes with $OPPh_3$ ligands were synthesized from the precursors containing a coordinated $OPPh_3$ ligand like $[ReOCl_3(Me_2S)(OPPh_3)]$.[4,10,22,23]

X-Ray Crystal Structures. X-ray crystal analyses revealed the presence of a complex molecule and a CH_2Cl_2 molecule (**1**) and only a complex molecule (**3** and **4**) in an asymmetric unit. Perspective drawings of the complex molecules **1** and **3** are shown in Figs. 1 and 2. Selected bond distances and angles for **1**, **3**, and **4** are listed in Tables 1 and 2. The coordination geometry around the Re atom in **1** is a distorted octahedron with the oxo ligand, the unsymmetrical didentate-*N*,*N* ligand, two chloro ligands, and the PPh_3 ligand. The oxo ligand and the aromatic amido N2 atom lie along the axial direction, and the heterocyclic N1 atom, the P atom, and two *cis* Cl atoms occupy the equatorial plane. On the other hand, the $OPPh_3$ ligand in **3** and **4** occupies the *trans* position to the

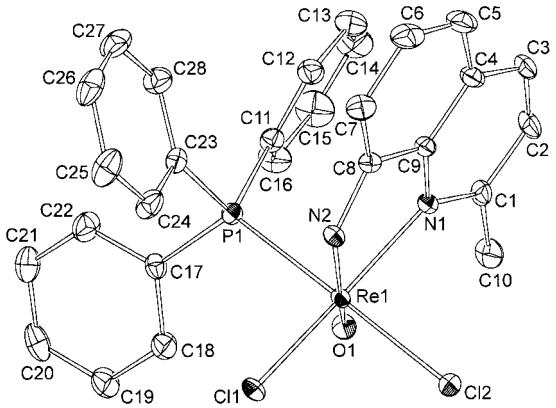

Fig. 1. An ORTEP view of $[ReOCl_2(Hamq)(PPh_3)]$ (**1**) with numbering scheme. Hydrogen atoms have been omitted for clarity.

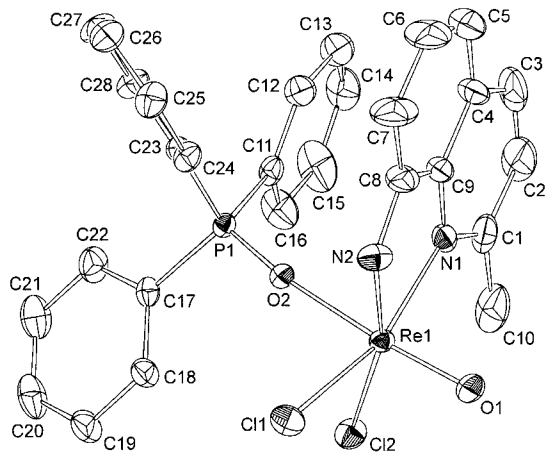

Fig. 2. An ORTEP view of $[ReOCl_2(Hamq)(OPPh_3)]$ (**3**) with numbering scheme. Hydrogen atoms have been omitted for clarity. The numbering scheme of $[ReOBr_2(Hamq)(OPPh_3)]$ (**4**) is the same as that of **3**.

Table 1. Selected Bond Distances (Å) and Angles (°) for $[ReOCl_2(Hamq)(PPh_3)]$ (**1**)

Re1–Cl1	2.337(1)	Re1–Cl2	2.452(1)
Re1–P1	2.455(1)	Re1–O1	1.724(4)
Re1–N1	2.165(4)	Re1–N2	1.999(4)
Cl1–Re1–Cl2	87.46(5)	Cl1–Re1–P1	92.43(5)
Cl1–Re1–O1	103.9(1)	Cl1–Re1–N1	161.0(1)
Cl1–Re1–N2	86.9(1)	Cl2–Re1–P1	178.34(5)
Cl2–Re1–O1	96.0(1)	Cl2–Re1–N1	87.7(1)
Cl2–Re1–N2	95.0(1)	P1–Re1–O1	82.4(1)
P1–Re1–N1	92.9(1)	P1–Re1–N2	86.6(1)
O1–Re1–N1	94.8(2)	O1–Re1–N2	164.9(2)
N1–Re1–N2	75.3(2)		

Table 2. Selected Bond Distances (Å) and Angles (°) for $[ReOX_2(Hamq)(OPPh_3)]$ (X = Cl, **3**; Br, **4**)

	3	**4**		**3**	**4**
Re1–X1	2.363(2)	2.509(1)	Re1–X2	2.447(2)	2.600(1)
Re1–O1	1.670(5)	1.665(7)	Re1–O2	2.116(4)	2.125(7)
Re1–N1	2.156(6)	2.170(10)	Re1–N2	1.952(7)	1.938(9)
X1–Re1–X2	85.77(9)	86.54(5)	X1–Re1–O1	102.6(2)	101.7(3)
X1–Re1–O2	87.7(1)	87.5(2)	X1–Re1–N1	162.5(2)	161.3(3)
X1–Re1–N2	87.5(2)	86.6(3)	X2–Re1–O1	92.6(2)	91.2(3)
X2–Re1–O2	80.9(1)	81.3(2)	X2–Re1–N1	103.9(2)	105.0(3)
X2–Re1–N2	163.8(2)	164.3(3)	O1–Re1–O2	167.4(2)	167.9(4)
O1–Re1–N1	91.6(2)	92.9(4)	O1–Re1–N2	103.3(3)	104.0(4)
O2–Re1–N1	79.7(2)	80.0(3)	O2–Re1–N2	84.2(2)	84.3(3)
N1–Re1–N2	79.2(3)	78.5(4)	Re1–O2–P1	167.6(3)	166.7(5)

oxo ligand, although the PPh_3 ligand in **1** occupies the *cis* position. This means that the coordination geometrical conversion occurred during the ligand substitution reaction of PPh_3 with $OPPh_3$. A similar tendency, in which the *trans* position of the oxo ligand prefers coordination of the oxygen atom, as observed in **3** and **4**, was generally observed for analogous $OPPh_3$ complexes.[9,22,23]

Although the Re–N1 distances in **1**, **3**, and **4** are within reported Re–N(heterocyclic) distances in oxorhenium(V) complexes (2.11–2.17 Å),[6–10,24] the Re–N2 distances are significantly shorter than the Re–N1 distances. Since the Re–N(amido) distances are in the range of 1.93 to 2.05 Å, it is suggested that the N2 amino group is partially deprotonated and the Re–N2 bond has a multi bond character between single and double bonds.[14–16] The Re=O distance in **1**, which occupies the *trans* position to the Re–N2(amido) bond, lies at the long end of the range found for the Re=O double bond in oxorhenium(V) complexes (1.63–1.71 Å).[6,7,14,24–27] On the other hand, the Re=O distances in **3** and **4**, which occupy the *trans* position to the $OPPh_3$ ligand, are normal for oxorhenium(V) complexes. Refosco et al. reported that the oxorhenium(V) complex $[ReO\{PPh_2(C_6H_4NH\text{-}2)\}_2Cl]$ has a surprisingly long Re=O bond (1.767(7) Å), which also occupies the *trans* position to the partially deprtotonated aromatic amido.[15] It is suggested, therefore, that the reason for the long Re=O bond in **1** is the result of the *trans* influence of the Re–N2(amido) bond. These characteristics are similar to those in the bis Haq complex $[ReO(Haq)_2(PPh_3)]^+$.[14] In addition, the Re–Cl2 distance in **3** is 0.084 Å longer than the Re–Cl1 distance because of the *trans* influence of the Re–N2(amido) bond. The *trans* influence of the P atom is also observed in **1**. The Re–Cl2 distance, which occupies the *trans* position to the P atom, is 0.115 Å longer than the Re–Cl1 distance, which occupies the *cis* position to the P atom. Similar behavior was also observed for the Re(V) complexes with phosphine ligands.[7,24,28,29] The bond distances and angles in **4** are approximately the same as those of **3**, except that the Re–Br distances are ca. 0.15 Å longer than the Re–Cl distances (Table 2), depending on the covalent bond radii.

In the cases of both **1** and **3**, the C11–C16 phenyl rings of the phosphine ligand are approximately parallel to the quinoline rings (dihedral angle = 22.7(2)° in **1** and 10.8(3)° in **3**) and the inter-ring average distances are 3.67(1) and 3.75(2) Å, respectively. In addition, the C11–C16 phenyl ring position is not just above the amq ring (torsion angle; N1–Re1–P1–C11 = −29.7(2)° in **1**), but it is over between the methyl group C10 and the edge of the quinoline ring C1. Consequently, it is suggested that intramolecular π–π and/or CH–π stacking interactions exist between these two planes.[22] This behavior is different from the mono aq complex $[ReCl_3(aq)(PPh_3)]$, where the phenyl ring is just above the quinoline ring.[20] This difference can be attributed to the presence of a substitution group. The intermolecular interactions are also considered to be a factor in the crystal packings of the representative complexes **1** and **3** (Fig. 3). In the crystal packing of **1**, quinoline rings of adjacent molecules are overlapping in the axial direction, and the complex molecules assume a dimeric structure. The interplane distances (average 3.46(8) Å) between the two planes of the neighboring amq moieties are within the range of intermolecular π–π stacking.[30,31] Although the CH_2Cl_2 molecule is also incorporated in the crystal packing, it does not participate in any intermolecular interactions. On the other hand, in the crystal packing of **3**, the molecules align according to the Re=O axis and no intermolecular π-π interaction is observed. The crystal packing of **4** is almost the same as that of **3**. Consequently, this seems to indicate that the differences in coordination geometry influence the crystal packing.

Spectroscopic Characterization. The IR spectral patterns of **1** and **2** are very similar to each other, and those of **3** and **4**, which gave the same geometrical structure in the X-ray analysis, are also similar to each other (Fig. 4). The band at ca. 3300 cm^{-1} due to the N–H bond supports the idea of a partially deprotonated amido group. The strong IR bands of the Re=O bond in **3** and **4** are observed at ca. 970 cm^{-1}, which are in the normal region (1000–940 cm^{-1}) for the analogous oxorhenium(V) complexes.[32] On the other hand, **1** and **2** exhibit the same IR bands at ca. 910 cm^{-1} on the lower wavenumber side. Since the lower wavenumber shift supports the long Re=O bond observed in the X-ray crystal analysis, it can be inferred that the structure of **2** should be similar to that of **1**. The large differences between the PPh_3 complexes and the $OPPh_3$ complexes are also observed at ca. 1150, 1120, and 725 cm^{-1}. These bands, which were only observed in **3** and **4**, seem to have arisen from the $OPPh_3$ ligand, since the free $OPPh_3$ ligand exhibits bands at 1190, 1120, and 722 cm^{-1}. In the far-IR spectra, the Re–Cl stretching bands in **1**

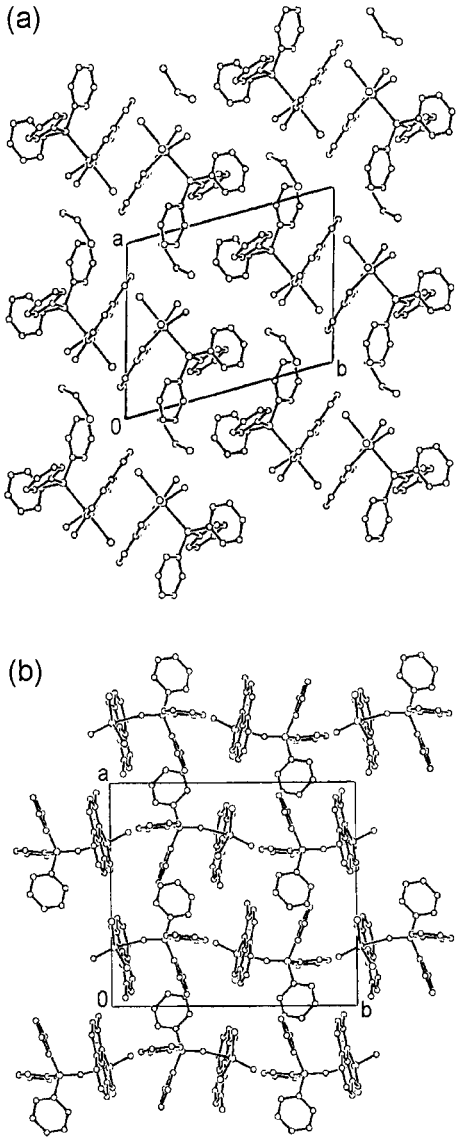

Fig. 3. Projection of crystal packings for (a) $[ReOCl_2(Hamq)(PPh_3)]\cdot CH_2Cl_2$ (**1**·CH_2Cl_2) and (b) $[ReOCl_2(Hamq)(OPPh_3)]$ (**3**) viewed along *c* axis.

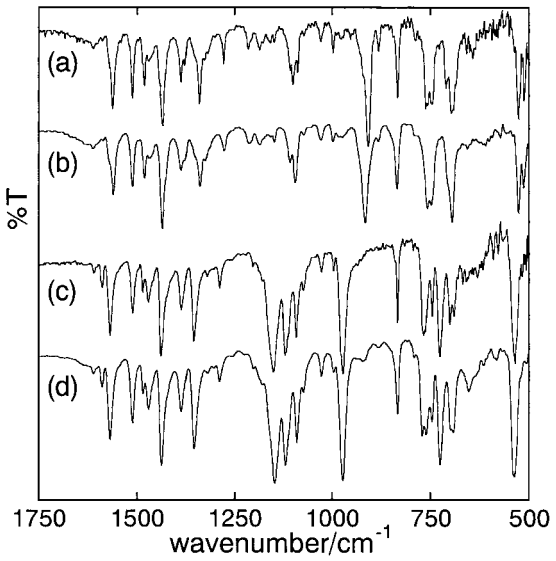

Fig. 4. IR spectra of (a) $[ReOCl_2(Hamq)(PPh_3)]$ (**1**), (b) $[ReOBr_2(Hamq)(PPh_3)]$ (**2**), (c) $[ReOCl_2(Hamq)(OPPh_3)]$ (**3**), and (d) $[ReOBr_2(Hamq)(OPPh_3)]$ (**4**).

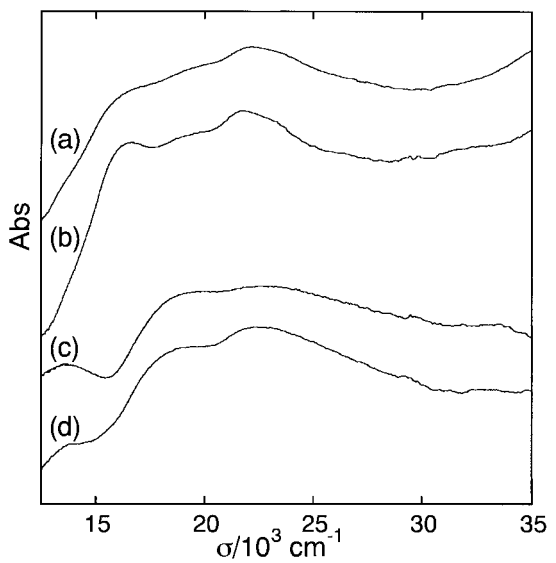

Fig. 5. Diffuse reflectance spectra of (a) $[ReOCl_2(Hamq)(PPh_3)]$ (**1**), (b) $[ReOBr_2(Hamq)(PPh_3)]$ (**2**), (c) $[ReOCl_2(Hamq)(OPPh_3)]$ (**3**), and (d) $[ReOBr_2(Hamq)(OPPh_3)]$ (**4**).

and **3** are observed at ca. 320 and 280 cm^{-1} as two strong bands. Although no strong bands are observed in **2** and **4** below 400 cm^{-1}, it is reasonable to assume that two relatively weak bands at ca. 230 and 210 cm^{-1} for **2** and **4** are due to the Re–Br stretching vibration mode by considering the reduced mass. Thus, **1**–**4** can be distinguished by the IR and far-IR spectra.

The solid state diffuse reflectance (DR) spectral patterns of **1** and **2** are similar to each other, and those of **3** and **4** are also similar to each other (Fig. 5). These reflect the structural similarities of the complexes. The representative UV-vis absorption spectra of the chloro complexes **1** and **3**, which were measured in a CH_2Cl_2 solution at various concentrations, are shown in Fig. 6. In the energy region lower than 27×10^3 cm^{-1}, the absorption spectra exhibit a concentration dependence, especially in **1**. The absorption spectrum of **1** in concentrated solution is relatively similar to its DR spectrum, whereas that in dilute solution is similar to the corresponding absorption spectrum of **3** rather than the DR spectrum of **1**. In **3**, the absorption spectra of the concentrated solution and the dilute one are similar to each other, and differ from the DR spectrum of **3**. Accordingly, **1** in dilute solution and **3** in concentrated and dilute solutions do not retain the structure observed in the X-ray analysis. Moreover, it is believed that they have an analogous structure which releases the PPh_3 or $OPPh_3$ ligand from each other. This is supported by the spectra of solutions containing **1** or **3** (ca. 10^{-5} mol dm^{-3}) and a large excess of PPh_3 (ca. 10^{-3} mol dm^{-3}) being similar to that of **1** in concentrated solution. In all cases, Fig. 6 shows characteristic bands at ca. 30×10^3 cm^{-1}. Although these bands appear in

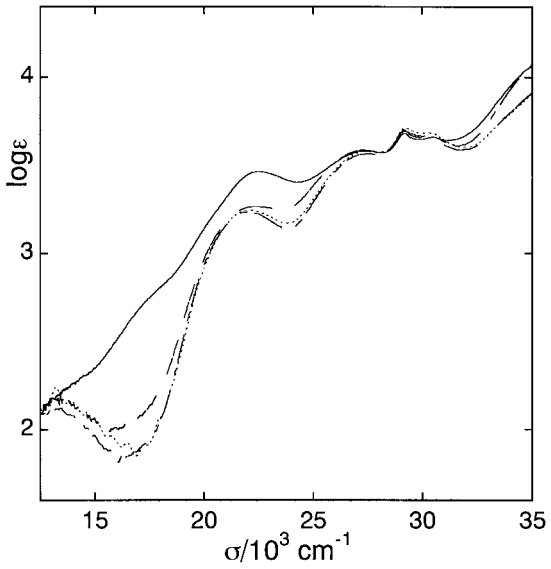

Fig. 6. UV-vis absorption spectra in CH_2Cl_2 of **1** in concentrated solution (2.99×10^{-3} mol dm^{-3}; —), **1** in dilute solution (5.63×10^{-5} mol dm^{-3}; – – –), **3** in concentrated solution (2.54×10^{-3} mol dm^{-3}; – – –), and **3** in dilute solution (1.69×10^{-5} mol dm^{-3}; - - - - -).

the region where the CT transition of the coordinated phosphine or quinoline ligands is normally observed,[15] these bands can be attributed to the coordinated amq ligand, considering the release of the phosphine. Similar results were observed for the bromo complexes **2** and **4**.

In $CDCl_3$ solution, a single $^{31}P\{^1H\}$ NMR signal was observed at δ −7.6 (**1**), −7.5 (**2**), 27.8 (**3**), and 27.7 (**4**). These are close to the values of the free PPh_3 (δ −7.4) and $OPPh_3$ (δ 27.4) ligands, implying the release of the ligand. Moreover, no signals due to the complex could be observed, even in a solution containing a large excess of PPh_3 or $OPPh_3$. The ^1H NMR spectra in solution could not be deciphered due to the dissociation of the ligand. For comparison, the measurements of the $^{31}P\{^1H\}$ CP-MAS NMR spectra in the solid state were carried out. The $^{31}P\{^1H\}$ CP-MAS NMR spectra for **3** and **4** exhibit many sharp signals with relatively low integration values (Fig. 7). Changing the spin rate establishes the distinction between many spinning-sidebands and one main signal at ca. 39 ppm for **3** and **4**. On the other hand, those for **1** and **2** show very broad signals, in spite of 6000 scans for integration, and could not be resolved. This broadening probably comes from some quadrupole interaction of Re ($I = 5/2$). In **1** and **2**, the P atom bonds to the Re atom directly, whereas the O atom exists between the P and Re atoms in **3** and **4**. Therefore, the $OPPh_3$ complexes do not undergo the corresponding interaction, as in **1** and **2**, and show sharp signals. A similar tendency was also observed for their precursors; $[ReOX_3(PPh_3)_2]$ (X = Cl or Br) showed broad signals, although the free PPh_3 and $OPPh_3$ ligands showed sharp signals. The sharp signal at ca. 40 ppm in **1** is expected to come from **3**, which is slightly introduced as an impurity. Consequently, it was elucidated that the $^{31}P\{^1H\}$ CP-MAS NMR spectra can be used for discriminating the presence of a direct Re–P bond or not. Additionally, the $^{31}P\{^1H\}$ spectra also supported the fact that the crystal

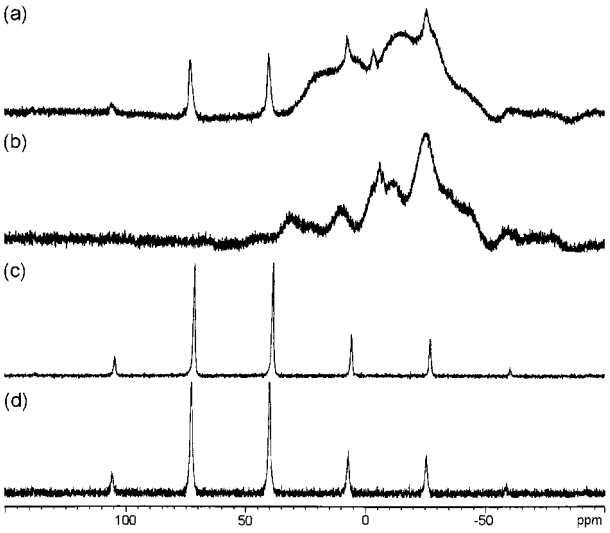

Fig. 7. $^{31}P\{^1H\}$ CP-MAS NMR spectra (spinning rate; 8000 rotation s^{-1}) of (a) $[ReOCl_2(Hamq)(PPh_3)]$ (**1**), (b) $[ReOBr_2(Hamq)(PPh_3)]$ (**2**), (c) $[ReOCl_2(Hamq)(OPPh_3)]$ (**3**), and (d) $[ReOBr_2(Hamq)(OPPh_3)]$ (**4**): 6000 times of integration for **1** and **2**, 64 times integration for **3** and **4**.

structures of **1**–**4** are not retained in solution.

Conclusion

In this work, two types of new oxorhenium(V) complexes with 2-methylquinolin-8-ylamido, which show interconversion with a coordination geometrical change, were prepared. They were characterized by X-ray crystallography, IR, UV-vis, and $^{31}P\{^1H\}$ NMR spectroscopic methods. It turned out that the present oxorhenium(V) complexes have much higher PPh_3 or $OPPh_3$ replacement ability than many reported oxorhenium (V) complexes. Because of this property, free coordination sites can be obtained easily. Further investigation of the replacement reactions using many neutral monodentate ligands is now in progress.

Experimental

Materials. Rhenium, 8-amino-2-methylquinoline (H_2amq), and triphenylphosphine oxide ($OPPh_3$) were purchased from Soekawa Chemical Co., Ltd., Tokyo Kasei Kogyo Co., Ltd., and Aldrich Chemical Co., Inc., respectively. The other materials were purchased from Wako Pure Chemical Ind., Ltd. All the chemicals were used without further purification. The starting materials $[ReOCl_3(PPh_3)_2]$ and $[ReOBr_3(PPh_3)_2]$ were prepared by the general procedure from perrhenate and triphenylphosphine (PPh_3).[33]

Preparation of Complexes. $[ReOCl_2(Hamq)(PPh_3)]$ (1): To a suspension containing $[ReOCl_3(PPh_3)_2]$ (515 mg, 0.618 mmol) in CH_2Cl_2 (35 cm^3) was added a solution containing H_2amq (190 mg, 1.20 mmol) in $C_6H_5CH_3$ (15 cm^3). The light green mixture was stirred for 1 h, whereupon the suspension turned to dark brown. After removing yellow insoluble materials (mainly H_3amqCl) by filtration, the filtrate was concentrated to 10 cm^3 under vacuum. The resulting dark brown precipitate was collected by filtration and washed with H_2O and Et_2O. Yield: 314 mg (73.3%). The precipitate was recrystallized from CH_2Cl_2/$C_6H_5CH_3$ to yield dark brown prismatic crystals (**1**, major product) and dark brown octahedral crystals (**3**, minor product). **3**

can be removed to a certain extent by washing with EtOH. Anal. Found: C, 48.54; H, 3.32; N, 4.15%. Calcd for [$ReOCl_2(C_{10}H_9N_2)P(C_6H_5)_3$]: C, 48.56; H, 3.49; N, 4.04%. IR 3292m (N–H) and 908s (Re=O) cm^{-1}. Far IR 334s and 270s (Re–Cl) cm^{-1}. DR 16.5sh, 19.1sh, 22.2 × 10^3 cm^{-1}. The sh label denotes a shoulder. H_3amqCl was also obtained by the treatment of H_2amq with HCl. This was confirmed by elemental analysis and IR spectra.

[$ReOBr_2$(Hamq)(PPh_3)] (2): The bromo complex **2** was synthesized by a similar method to the chloro complex **1**. To a suspension containing [$ReOBr_3(PPh_3)_2$] (500 mg, 0.517 mmol) in CH_2Cl_2 (130 cm^3) was added a solution containing H_2amq (160 mg, 1.01 mmol) in $C_6H_5CH_3$ (20 cm^3). The yellow mixture was stirred for 1 h, whereupon the suspension turned to dark brown. After removing insoluble materials, the filtrate was concentrated to 10 cm^3 under vacuum. A dark brown precipitate appeared. Yield: 331 mg (81.9%). The precipitate was recrystallized from $CH_2Cl_2/C_6H_5CH_3$ to yield dark brown microcrystals (**2**, major product) and dark brown octahedral crystals (**4**, minor product). Anal. Found: C, 42.52; H, 2.93; N, 3.83%. Calcd for [$ReOBr_2(C_{10}H_9N_2)P(C_6H_5)_3$]: C, 43.03; H, 3.10; N, 3.58%. IR 3254m (N–H) and 915s (Re=O) cm^{-1}. Far IR 224w and 202w (Re–Br) cm^{-1}. DR 16.6, 19.1sh, 21.7 × 10^3 cm^{-1}. **1** and **2** are soluble in CH_2Cl_2 and $CHCl_3$, slightly soluble in EtOH, and insoluble in H_2O and Et_2O.

[$ReOCl_2$(Hamq)($OPPh_3$)] (3): To a solution containing **1** (90.2 mg, 0.130 mmol) in the mixed solvent of CH_2Cl_2 (60 cm^3) and $C_6H_5CH_3$ (10 cm^3) was added $OPPh_3$ (383 mg, 1.38 mmol) and stirred for 10 min. The dark brown solution was filtered to remove insoluble materials and the filtrate was concentrated to 10 cm^3 under vacuum. After the resulting brown precipitate was collected by filtration and washed with Et_2O, the precipitate was redissolved in the mixed solvent of CH_2Cl_2 (60 cm^3) and $C_6H_5CH_3$ (10 cm^3). To this solution was added $OPPh_3$ (370 mg, 1.33 mmol), filtered, and concentrated to 10 cm^3 under vacuum again. The resulting reddish brown precipitate was filtered and washed with a small amount of EtOH and Et_2O. Yield: 57.6 mg (62.5%). Anal. Found: C, 47.51; H, 3.47; N, 3.85%. Calcd for [$ReOCl_2(C_{10}H_9N_2)OP(C_6H_5)_3$]: C, 47.46; H, 3.41; N, 3.95%. IR 3316m (N–H) and 973s (Re=O) cm^{-1}. Far IR 316s and 280s (Re–Cl) cm^{-1}. DR 13.6, 19.9, 22.7 × 10^3 cm^{-1}. $^{31}P\{^1H\}$ CP-MAS NMR δ 38.4.

[$ReOBr_2$(Hamq)($OPPh_3$)] (4): The bromo complex **4** was synthesized by a similar method to the chloro complex **3**. After **2** (98.2 mg, 0.126 mmol) was reacted with $OPPh_3$ (360 mg, 1.29 mmol) in the mixed solvent of CH_2Cl_2 and $C_6H_5CH_3$, the reaction mixture was concentrated under vacuum. The resulting brown precipitate was redissolved in the mixed solvent and reacted with $OPPh_3$ again. After the solution was concentrated, a reddish brown precipitate appeared. Yield: 42.3 mg (42.1%). Anal. Found: C, 42.14; H, 2.87; N, 3.65%. Calcd for [$ReOBr_2(C_{10}H_9N_2)OP(C_6H_5)_3$]: C, 42.17; H, 3.03; N, 3.51%. IR 3311m (N–H) and 972s (Re=O) cm^{-1}. Far IR 231w and 210w (Re–Br) cm^{-1}. DR 13.8sh, 19.2sh, 22.5 × 10^3 cm^{-1}. $^{31}P\{^1H\}$ CP-MAS NMR δ 39.7. **3** and **4** are soluble in CH_2Cl_2, $CHCl_3$, and EtOH, and insoluble in H_2O and Et_2O.

Reaction of [$ReOX_2$(Hamq)($OPPh_3$)] with PPh_3. To a solution containing **3** (20.6 mg, 0.0291 mmol) in the mixed solvent of CH_2Cl_2 (20 cm^3) and $C_6H_5CH_3$ (5 cm^3) was added PPh_3 (76.4 mg, 0.291 mmol). The dark brown solution was stirred for 15 min and concentrated to 5 cm^3 under vacuum. The resulting dark brown precipitate of **1** was collected by filtration and washed with Et_2O. Yield: 9.7 mg (48%). **2** was also obtained by the same method using **4** (20.4 mg, 0.0260 mmol) and PPh_3 (68.4 mg, 0.261 mmol). Yield: 12.7 mg (63.6%). These were confirmed by IR spectra.

Measurements. Elemental analyses (C, H, N) were performed by the Chemical Analysis Center of the University of Tsukuba. IR and far-IR spectra were recorded on a JASCO FT/IR-550 spectrometer as KBr pellets and Nujol mulls between polyethylene plates, respectively. UV-vis absorption spectra were recorded on a JASCO V-560 spectrophotometer. Diffuse reflectance spectra were recorded on a JASCO V-570 spectrophotometer equipped with an integrating sphere apparatus (JASCO ISN-470) using powder

Table 3. Crystal Data and Experimental Parameters for [$ReOCl_2$(Hamq)(PPh_3)]·CH_2Cl_2 (**1**·CH_2Cl_2), [$ReOCl_2$(Hamq)($OPPh_3$)] (**3**), and [$ReOBr_2$(Hamq)($OPPh_3$)] (**4**)

	1·CH_2Cl_2	**3**	**4**
Formula	$C_{29}H_{26}Cl_4N_2OPRe$	$C_{28}H_{24}Cl_2N_2O_2PRe$	$C_{28}H_{24}Br_2N_2O_2PRe$
Formula weight	777.53	708.60	797.50
Crystal system	triclinic	monoclinic	monoclinic
Space group	$P\bar{1}$ (No. 2)	$P2_1/n$ (No. 14)	$P2_1/n$ (No. 14)
a/Å	11.551(2)	14.90(1)	15.127(3)
b/Å	14.105(2)	17.272(4)	17.376(4)
c/Å	10.133(1)	10.485(2)	10.569(2)
α/°	91.258(9)		
β/°	109.252(10)	95.46(4)	96.56(2)
γ/°	75.30(1)		
V/Å^3	1504.2(3)	2685(2)	2759.6(10)
Z	2	4	4
D_{calcd}/g cm^{-3}	1.72	1.75	1.92
μ (Mo Kα)/cm^{-1}	44.7	48.1	74.0
Reflections collected, unique, R_{int}	7390, 6902, 0.018	6722, 6180, 0.037	6901, 6347, 0.038
Reflections used ($I > 1.5\sigma(I)$)	5824	4862	4058
Variable Parameters	343	325	325
Final $R(F^2)$, $R_w(F^2)$	0.053, 0.086	0.068, 0.106	0.074, 0.116
GOF	1.02	1.40	1.11

samples diluted by MgO. ^{1}H and ^{31}P{^{1}H} NMR spectra in $CDCl_3$ were obtained on a BRUKER AVANCE 600 spectrometer with $SiMe_4$ as an internal reference and PPh_3 as an external reference (in $CDCl_3$, PPh_3 resonates at δ −7.42 with respect to 85% H_3PO_4 in D_2O),[15] respectively. ^{31}P{^{1}H} CP-MAS NMR spectra were obtained at 243 MHz with the BRUKER AVANCE 600 spectrometer equipped with a PHMAS 4BL VTN instrument and $NH_4H_2PO_4$ as an external reference (δ 1.0).

Crystallography. Single crystals of **1**·CH_2Cl_2, **3**, and **4** were used for data collection on a Rigaku AFC-7S four-circle diffractometer with graphite-monochromatized Mo Kα (0.71069 Å) radiation. The unit-cell dimensions were determined by a least-squares refinement of 25 reflections. The intensity data were collected by the ω–2θ scan technique up to 55° at 296 K. The intensities were corrected for Lorentz and polarization. An empirical absorption correction based on a series of Ψ scans was applied. The crystal data and experimental parameters are listed in Table 3.

The positions of most non-hydrogen atoms were determined by a direct method (SIR 92)[34] and some remaining atoms positions were found by successive difference Fourier techniques.[35] The structures were refined by full-matrix least-squares techniques using anisotropic thermal parameters for non-hydrogen atoms. All the hydrogen atoms were included in the refinement but restrained to ride on the atoms (C–H = N–H = 0.95 Å, U(H) = 1.2U(C, N)). All of the calculations were performed using the teXsan crystallographic software package.[36] Crystallographic data have been deposited at the CCDC, 12 Union Road, Cambridge CB2 1EZ, UK and copies can be obtained on request, free of charge, by quoting the publication citation and the deposition numbers 185380–185382.

This work was supported by Grants-in-Aid for Scientific Research and COE Research from the Ministry of Education, Culture, Sports, Science and Technology.

References

1 W. A. Volkert and T. J. Hoffman, *Chem. Rev.*, **99**, 2269 (1999), and references therein.

2 C. Savoie and C. Reber, *Coord. Chem. Rev.*, **171**, 387 (1998).

3 J. B. Arterburn, M. C. Perry, S. L. Nelson, B. R. Dible, and M. S. Holguin, *J. Am. Chem. Soc.*, **119**, 9309 (1997).

4 M. M. Abu-Omar and S. I. Khan, *Inorg. Chem.*, **37**, 4979 (1998).

5 F. Connac, Y. Lucchese, M. Gressier, M. Dartiguenave, and A. L. Beauchamp, *Inorg. Chim. Acta*, **304**, 52 (2000).

6 J. M. Botha, K. Umakoshi, Y. Sasaki, and G. J. Lamprecht, *Inorg. Chem.*, **37**, 1609 (1998).

7 I. Chakraborty, S. Bhattacharyya, S. Banerjee, B. K. Dirghangi, and A. Chakravorty, *J. Chem. Soc., Dalton Trans.*, **1999**, 3747.

8 S. Bélanger and A. L. Beauchamp, *Inorg. Chem.*, **35**, 7839 (1996).

9 S. Bélanger and A. L. Beauchamp, *Inorg. Chem.*, **36**, 3640 (1997).

10 S. Fortin and A. L. Beauchamp, *Inorg. Chem.*, **39**, 4886 (2000).

11 S. Fortin and A. L. Beauchamp, *Acta Crystallogr., Sect. C*, **55**, 517 (1999).

12 J. C. Bryan, R. E. Stenkamp, T. H. Tulip, and J. M. Mayer, *Inorg. Chem.*, **26**, 2283 (1987).

13 J.-H. Jung, J.-S. Park, D. M. Hoffman, and T. R. Lee, *Polyhedron*, **20**, 2129 (2001).

14 M. T. Ahmet, B. Coutinho, J. R. Dilworth, J. R. Miller, S. J. Parrott, Y. Zheng, M. Harman, M. B. Hursthouse, and A. Malik, *J. Chem. Soc., Dalton Trans.*, **1995**, 3041.

15 F. Refosco, F. Tisato, G. Bandoli, C. Bolzati, A. Moresco, and M. Nicolini, *J. Chem. Soc., Dalton Trans.*, **1993**, 605.

16 G. Bandoli, A. Dolmella, T. I. A. Gerber, J. Perils, and J. G. H. du Preez, *Inorg. Chim. Acta*, **303**, 24 (2000).

17 H. Luo, I. Setyawati, S. J. Rettig, and C. Orvig, *Inorg. Chem.*, **34**, 2287 (1995).

18 M. Hirsch-Kuchma, T. Nicholson, A. Davison, W. M. Davis, and A. G. Jones, *Inorg. Chem.*, **36**, 3237 (1997).

19 G. Bandoli, T. I. A. Gerber, J. Perils, and J. G. H. du Preez, *Inorg. Chim. Acta*, **278**, 96 (1998).

20 Y. Miyashita, N. Mahboob, S. Tsuboi, Y. Yamada, K. Fujisawa, and K. Okamoto, *Acta Crystallogr., Sect. C*, **57**, 558 (2001).

21 Unpublished results.

22 L. Hansen, E. Alessio, M. Iwamoto, P. A. Marzilli, and L. G. Marzilli, *Inorg. Chim. Acta*, **240**, 413 (1995).

23 G. Battistuzzi, M. Cannio, M. Saladini, and R. Battistuzzi, *Inorg. Chim. Acta*, **320**, 178 (2001).

24 X. Chen, F. J. Femia, J. W. Babich, and J. Zubieta, *Inorg. Chim. Acta*, **308**, 80 (2000).

25 J. M. Mayer, D. L. Thorn, and T. H. Tulip, *J. Am. Chem. Soc.*, **107**, 7454 (1985).

26 T. I. A. Gerber, J. Bruwer, G. Bandoli, J. Perils, and J. G. H. du Preez, *J. Chem. Soc., Dalton Trans.*, **1995**, 2189.

27 C. Bolzati, F. Tisato, F. Refosco, G Bandoli, and A. Dolmella, *Inorg. Chem.*, **35**, 6221 (1996).

28 X. Chen, F. J. Femia, J. W. Babich, and J. Zubieta, *Inorg. Chim. Acta*, **306**, 113 (2000).

29 S. Bhattacharyya, S. Banerjee, B. K. Dirghangi, M. Menon, and A. Chakravorty, *J. Chem. Soc., Dalton Trans.*, **1999**, 155.

30 Y. Yamada, K. Fujisawa, and K. Okamoto, *Bull. Chem. Soc. Jpn.*, **73**, 2067 (2000).

31 Y. Yamada, K. Fujisawa, and K. Okamoto, *Bull. Chem. Soc. Jpn.*, **73**, 2297 (2000).

32 J. O'Neil, S. Wilson, and J. Katzenellenbogen, *Inorg. Chem.*, **33**, 319 (1994).

33 N. P. Johnson, C. J. L. Lock, and G. Wilkinson, *Inorg. Synth.*, **9**, 145 (1964).

34 A. Altomare, M. C. Burla, M. Camalli, M. Cascarano, C. Giacovazzo, A. Guagliardi, and G. Polidori, *J. Appl. Crystallogr.*, **27**, 435 (1994).

35 P. T. Beurskens, G. Admiraal, G. Beurskens, W. P. Bosman, R. de Gelder, R. Israel, and J. M. M. Smits, "DIRDIF 94, The DIRDIF-94 Program System, Technical Report of the Crystallography Laboratory", University of Nijmegen, The Netherlands (1994).

36 "teXsan. Single Crystal Structure Analysis Software, Version 1.10b." Molecular Structure Corporation, The Woodlands, TX, USA (1999).